

Supporting Information

Diameter and elasticity governing the relaxation of soft-nanoparticle melts

Jintian Luo[‡], Yihui Zhu[‡], Yifu Ruan[‡], Weiwei Wu[‡], Xikai Ouyang[‡],

Zhukang Du^{§,*}, GengXin Liu^{‡,*}

[‡]State Key Laboratory for Modification of Chemical Fibers and Polymer Materials, Center for Advanced Low-dimension Materials, College of Material Science and Engineering, Donghua University, Shanghai 201620, China

[§]South China Advanced Institute for Soft Matter Science and Technology, School of Molecular Science and Engineering, South China University of Technology, Guangzhou, 510640, China

- 1. DLS results (Figure S1 ~ S4)**
- 2. Flory-Rehner swelling model**
- 3. Glass transition temperature (Figure S5)**
- 4. WLF analysis (Figure S6)**
- 5. Discussion of modulus (Figure S7 ~ S8, Table S1)**
- 6. Creep data and converting into dynamic moduli (Figure S9 ~ S10)**
- 7. Degradation concerns (Figure S11)**
- 8. Fitting of equation 12 in the lin-log scale of Figure 6 (Figure S12)**
- 9. Alternative fitting of Figure 5a against the effective volume and in log-lin scale (Figure S13 ~ S15)**

1. DLS results

The intensity correlation function $G_2(\tau)$ is provided as the directly measured quantity. Then, a field correlation function $g_1(\tau)$ could be obtained

$$g_1(\tau) = \int_0^{+\infty} G(\Gamma) e^{-\Gamma\tau} d\Gamma$$

CONTIN method (installed in the instrument software) is used to perform the numerical inverse Laplace transformation on $g_1(\tau)$ to get $G(\Gamma)$. Then, momentums of Γ in order n

$$\langle \Gamma^n \rangle \equiv \int_0^{+\infty} \Gamma^n G(\Gamma) d\Gamma$$

Then, the measured averaged diameter is calculated by

$$\langle d_H \rangle \equiv \frac{q^2 k_B T}{3\pi\eta \langle \Gamma \rangle} = \frac{\alpha_q}{\langle \Gamma \rangle}$$

Polydispersity index

$$\mathfrak{D} \equiv \frac{\langle \Gamma^2 \rangle - \langle \Gamma \rangle^2}{\langle \Gamma \rangle^2} = \frac{\langle \Gamma^2 \rangle}{\langle \Gamma \rangle^2} - 1$$

A diameter variable based on a logarithmic scale

$$x \equiv \log d_H$$

Supposing a Gaussian distribution for diameter variable x

$$f(x) = \frac{1}{\sqrt{\pi}\sqrt{2\sigma^2}} \exp\left(-\frac{(x - \bar{x})^2}{2\sigma^2}\right)$$

$$G(\Gamma) = f(x) \frac{dx}{d\Gamma}$$

As a result, the momentum of Γ could be expressed with \bar{x} and σ^2

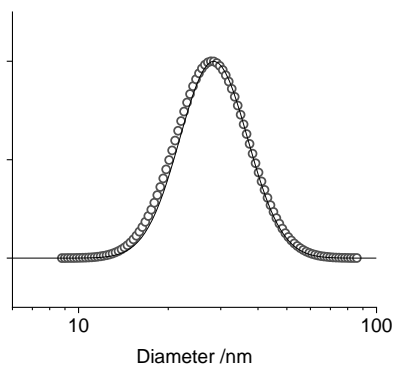
$$\langle \Gamma^n \rangle = \int_0^{+\infty} \Gamma^n f(x) \frac{dx}{d\Gamma} d\Gamma = \int_{-\infty}^{+\infty} \Gamma^n f(x) dx = \alpha_q^n \int_{-\infty}^{+\infty} 10^{-nx} f(x) dx = \alpha_q^n \cdot 10^{\frac{n^2 \sigma^2 \ln 10}{2} - n\bar{x}}$$

Combining with the definition of $\langle d_H \rangle$ and \mathfrak{D} , the gaussian distribution of size could be reconstructed with

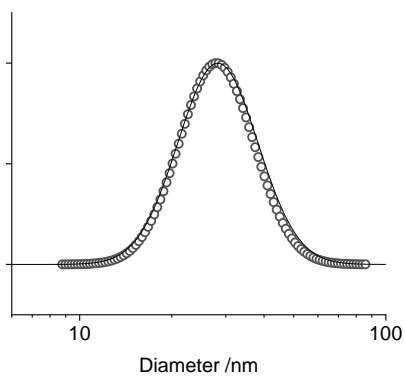
$$\bar{x} = \log \langle d_H \rangle + \frac{1}{2} \log(\mathfrak{D} + 1) \quad (S1)$$

$$\sigma^2 = \frac{1}{\ln 10} \log(\mathfrak{D} + 1) \quad (S2)$$

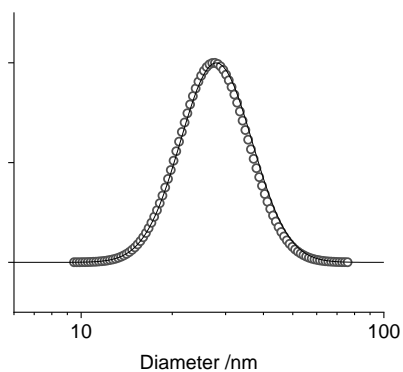
D17N100



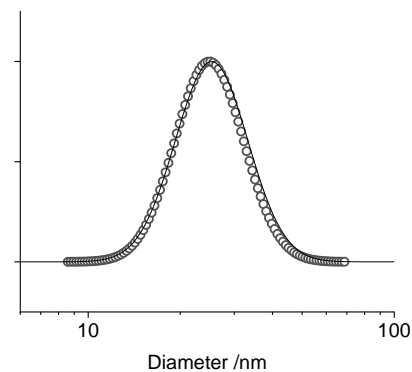
D17N40



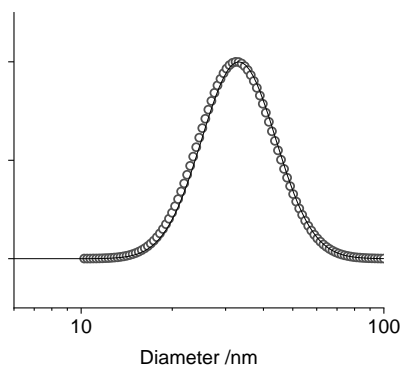
D17N80



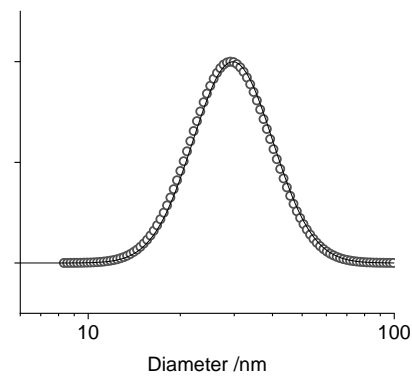
D15N80



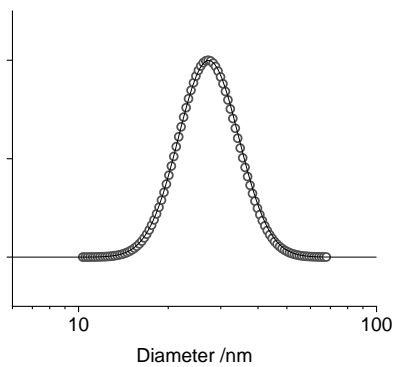
D32N60



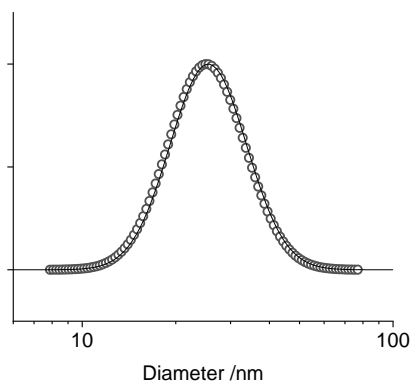
D18N60



D17N60



D15N60



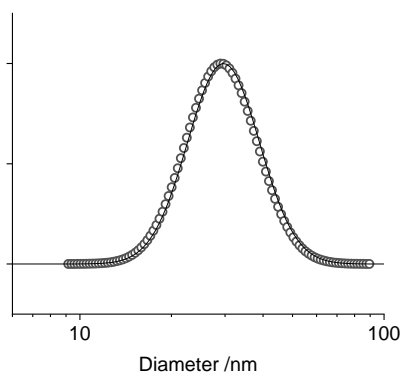
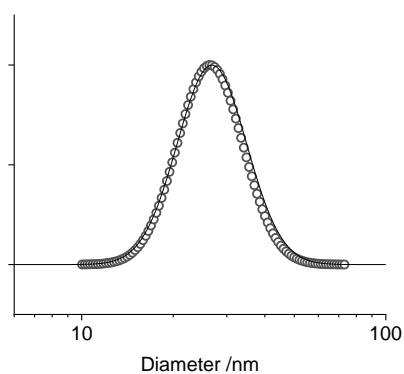
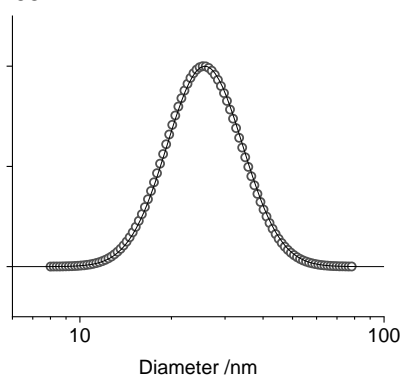
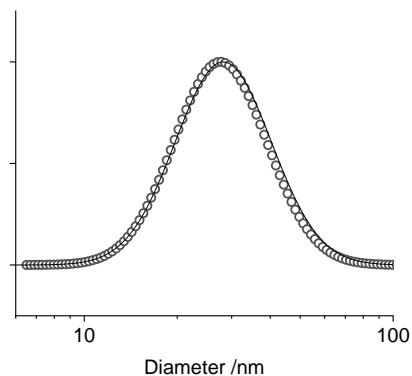
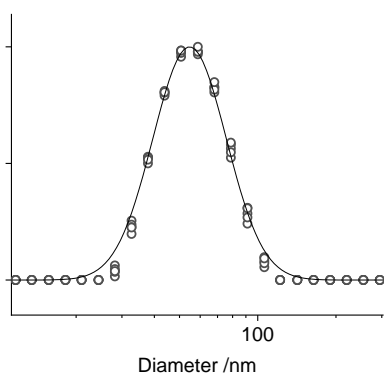
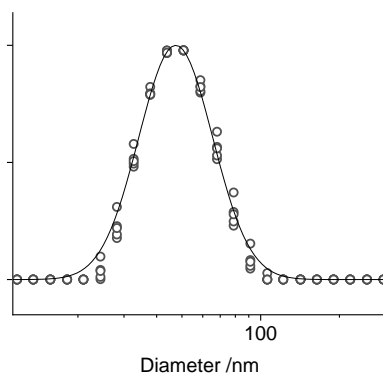
D18N50**D16N50****D16N05****D17N20**

Figure S1. The size distribution $f(x)$ of the microemulsion product in water, to determine D_{latex} . The solid curves were reconstructed with eq. (S1) and (S2)

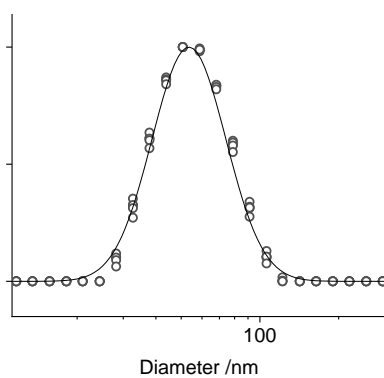
D17N100



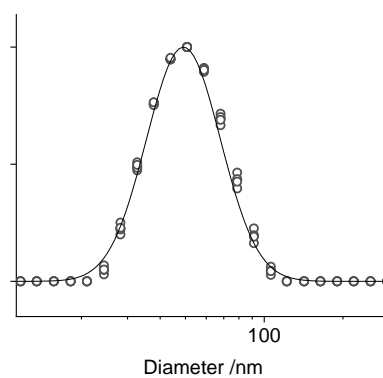
D17N40



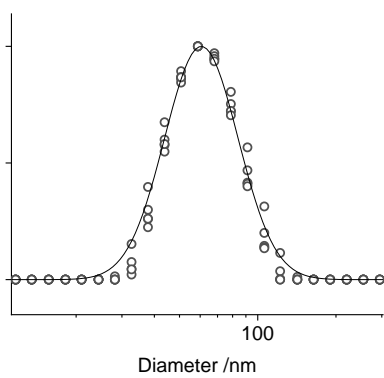
D17N80



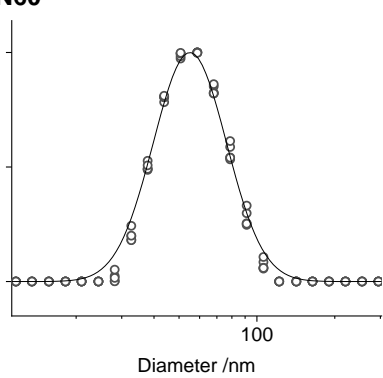
D15N80



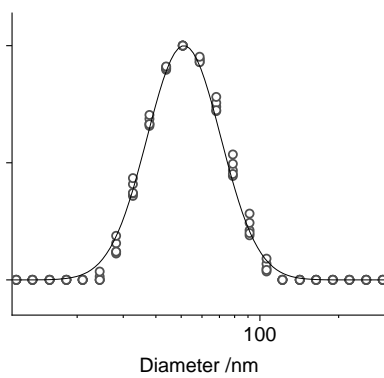
D20N60



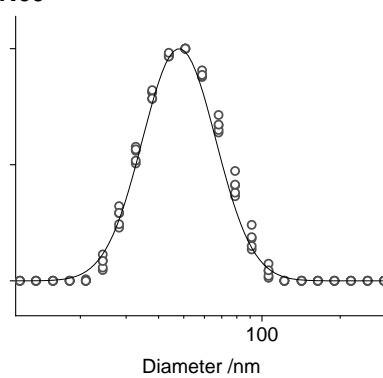
D18N60



D17N60



D15N60



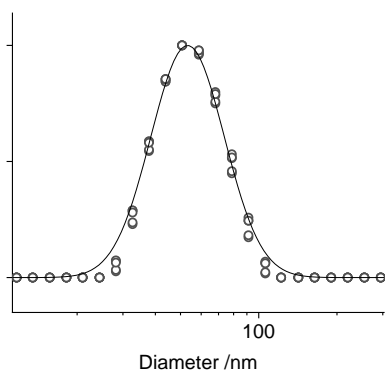
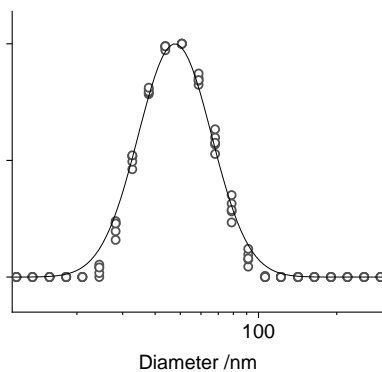
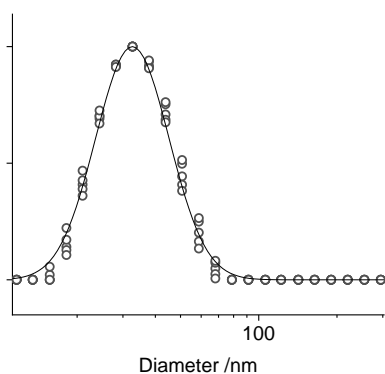
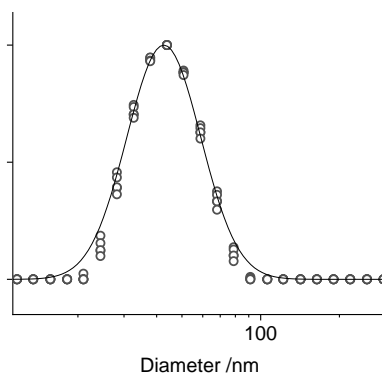
D18N50**D16N50****D16N05****D17N20**

Figure S2. The size distribution $f(x)$ of the purified SNP in THF, to determine D_{sw0} . The solid curves were reconstructed with eq. (S1) and (S2)

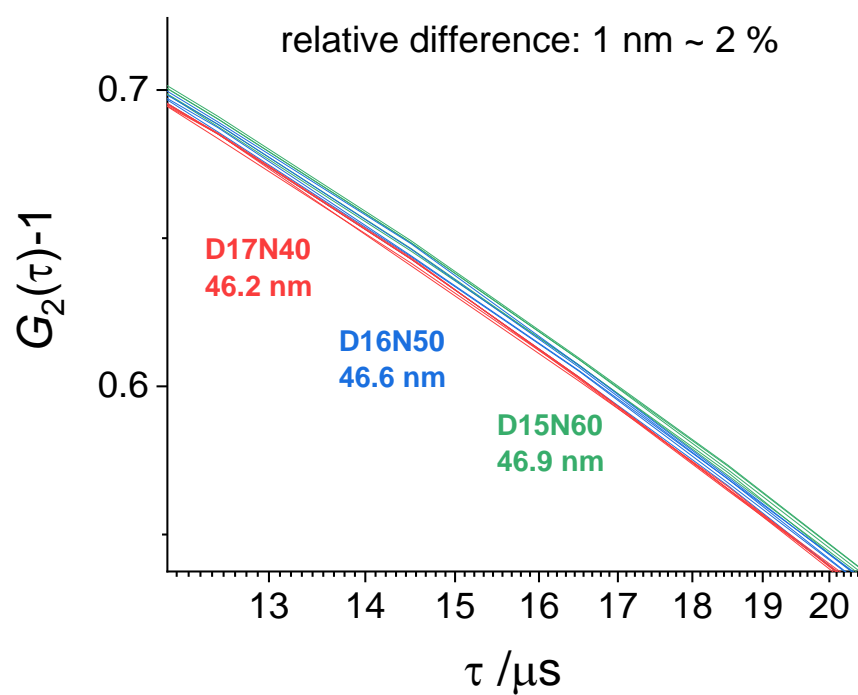
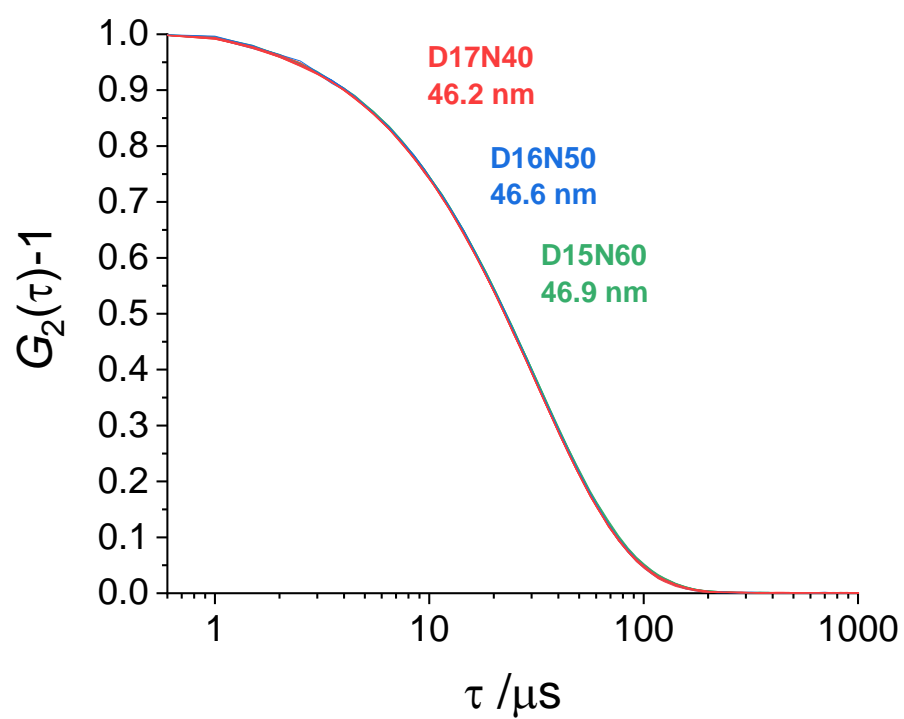


Figure S3. The upper graph is the intensity correlation function of three selected samples of which the difference of measured averaged-diameters is within 1nm. The lower graph is a zoom-in window of the upper graph. There would be observable diversity between these samples.

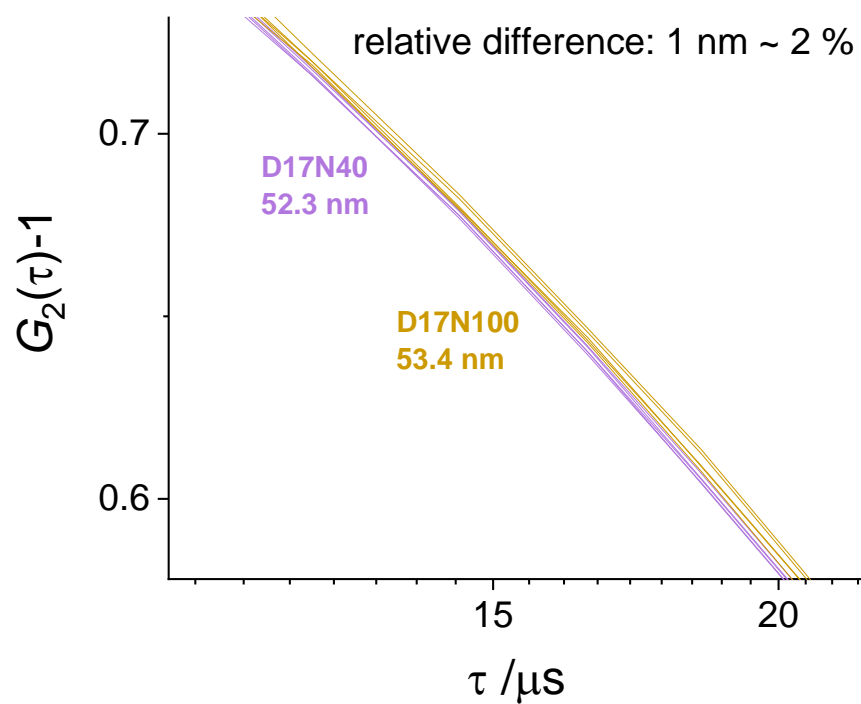
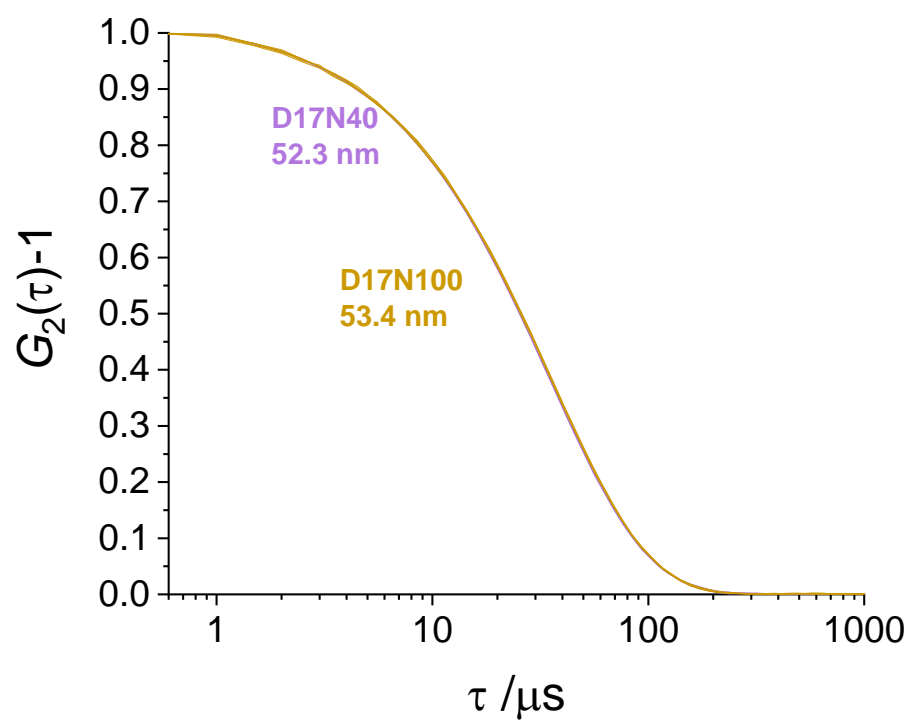


Figure S4. The upper graph is the intensity correlation function of another two selected samples of which the difference of measured averaged-diameters is about 1nm. The lower graph is a zoom-in window of the upper graph. There would be observable diversity between these samples.

2. Flory-Rehner swelling model

The swelling behavior was widely described by the Flory-Rehner model, which put forward a relation of the swelling ratio and the crosslinking degree N_c as

$$\frac{\varphi_0}{N_c} \left(\frac{\varphi}{2\varphi_0} - \left(\frac{\varphi}{\varphi_0} \right)^{1/3} \right) = \varphi + \ln(1 - \varphi) + \chi\varphi^2 .$$

In there, φ_0 is the polymer volume fraction of an initial state which is the bulk state in our discussion, and then

$$\varphi_0 = 1 ,$$

and the polymer volume fraction of the swollen state could be expressed with the swelling ratio

$$\varphi \approx \frac{1}{Q} .$$

Thus,

$$N_c = \frac{\left(\frac{1}{2Q} - Q^{-1/3} \right)}{Q^{-1} + \ln(1 - Q^{-1}) + \chi Q^{-2}}$$

The interaction parameter χ would be the only adjusted fitting parameter. However, this apparent interaction parameter for microgel was found rarely to match the widely studied Flory-Huggins parameter in linear polymer solutions (Soft Matt. – 13(2017), 8271 and the references inside).

The fitting in Figure 2 yields an apparent interaction parameter $\chi = -3.2$.

3. Glass transition temperature

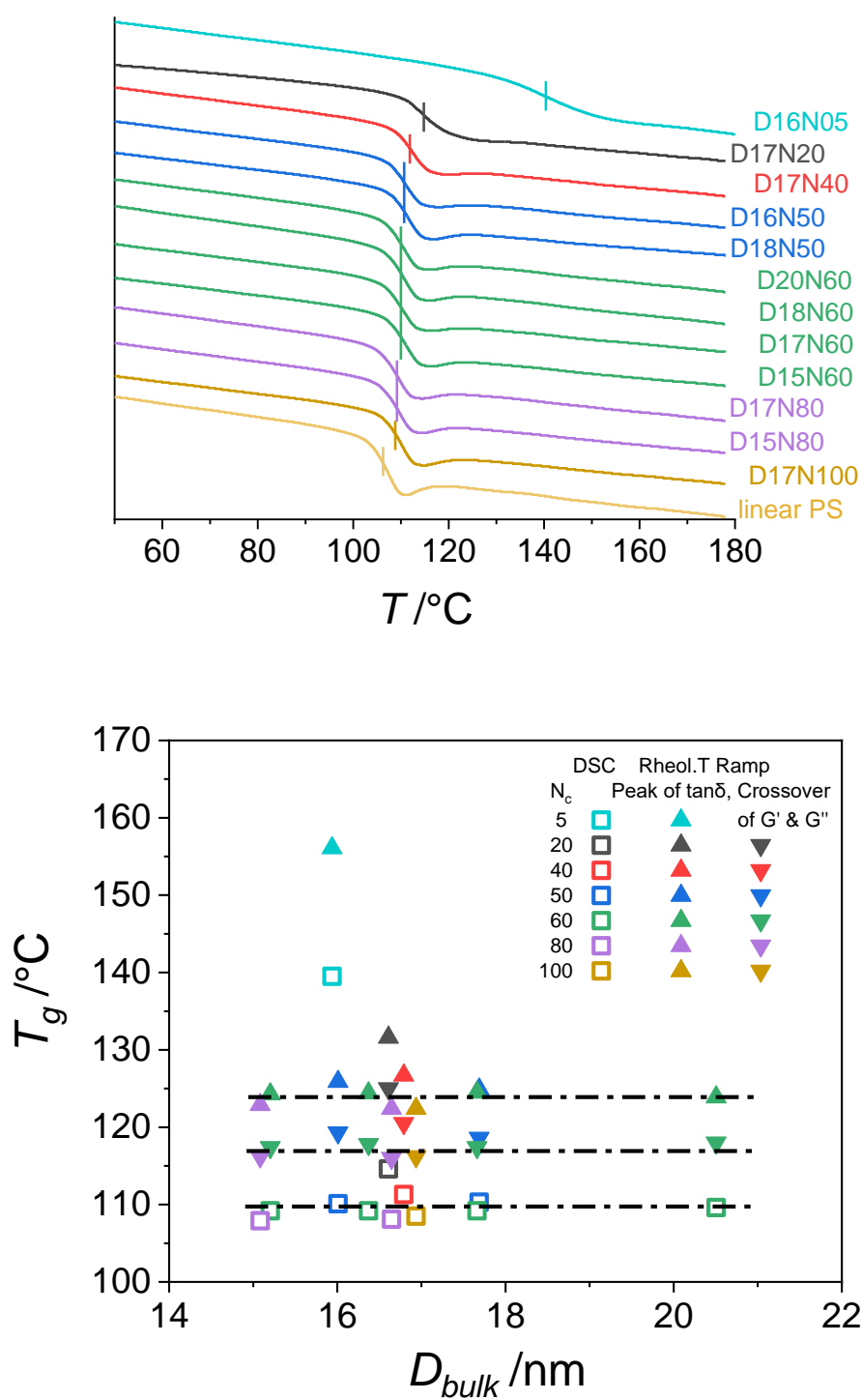


Figure S5. The upper graph is the results of DSC. The lower graph is the summarized T_g evaluated by DSC, $\tan \delta$ peak and crossover of G' and G'' of temperature ramp test.

4. WLF analysis

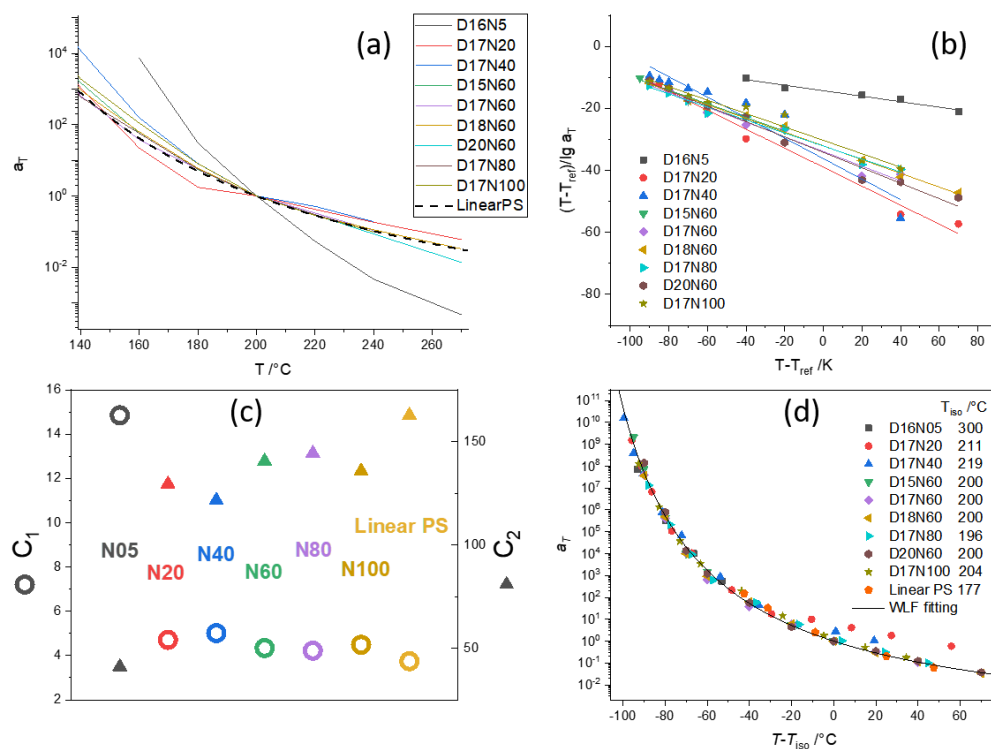


Figure S6. Fitting of horizontal shifting factor a_T according to WLF equation, plotted by (a) a_T - T and (b) normalized a_T and T . (c) Summary of C_1 and C_2 . (d) a_T replotted against temperature normalized by iso-friction temperature after applying WLF analysis (Macromolecules – 41(2008), 8694).

5. Discussion of modulus

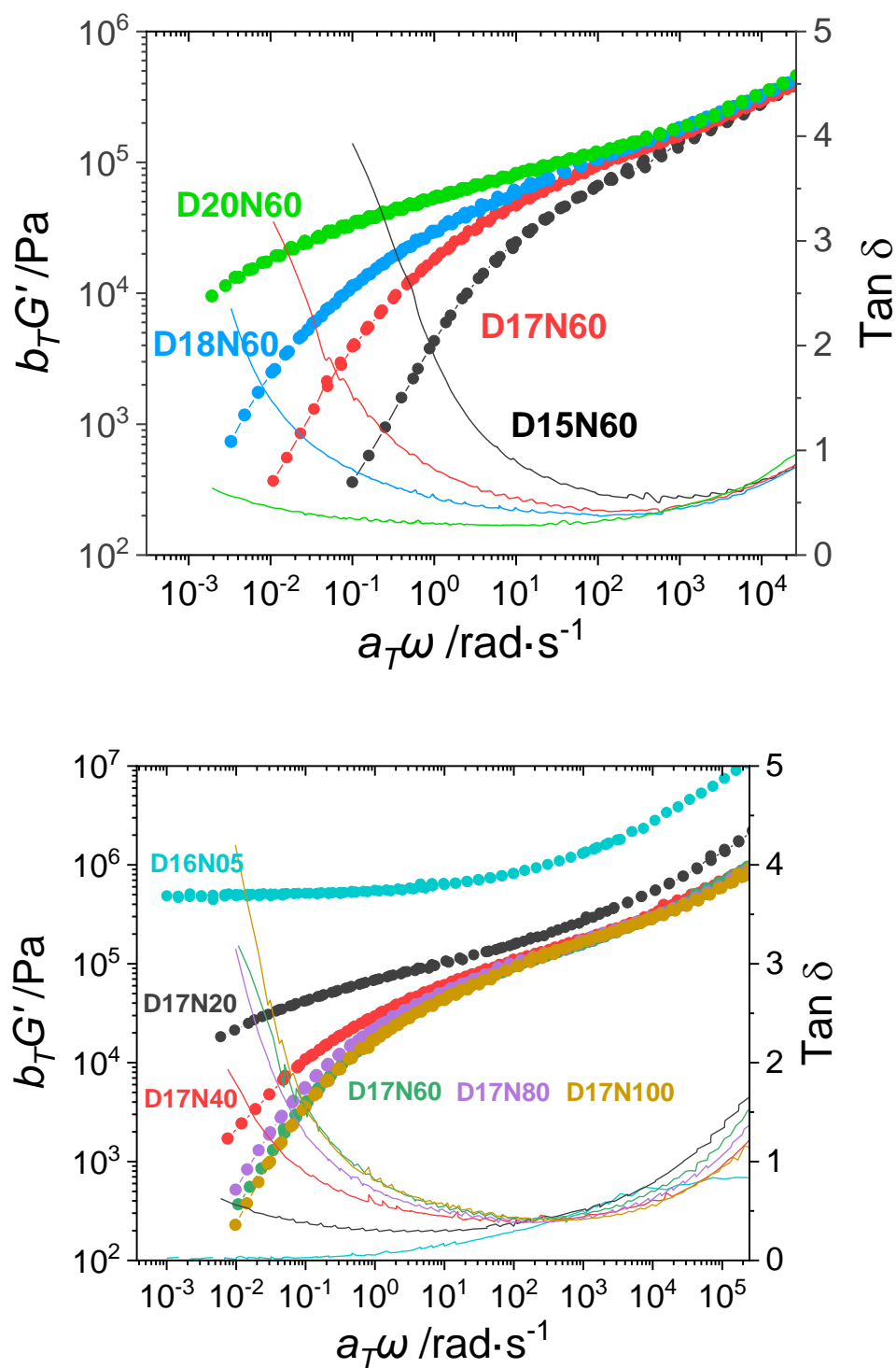


Figure S7. The storage modulus G' and $\tan \delta$ of SNP

Table S1. The modulus G' of SNP evaluated at the value of 1 and the minimum of $\tan \delta$ as shown in Figure S6

$\tan \delta$	1 (low freq.)	G' / Pa	
		minimum	1 (high freq.)
D20N60		90000	520000
D18N60	6500	120000	590000
D17N60	12000	110000	550000
D15N60	19000	110000	520000
D16N05		500000	
D17N20		90000	670000
D17N40	8000	120000	730000
D17N60	12000	110000	550000
D17N80	9500	120000	600000
D17N100	9000	120000	660000
LinearPS	50000	220000	600000

(1) The storage modulus G' of SNP except for D16N05 at the minimum of $\tan \delta$ and the high-frequency crossover point of the moduli shows no typical feature.

(2) The storage modulus G' of SNP at the low-frequency crossover point of the moduli shows a D_{bulk} -dependence. However, it lacks a clear dependence of N_c .

(3) The corresponding modulus of linear polystyrene ($\sim 1 \text{ M}$) would be higher than the SNP except for D16N05.

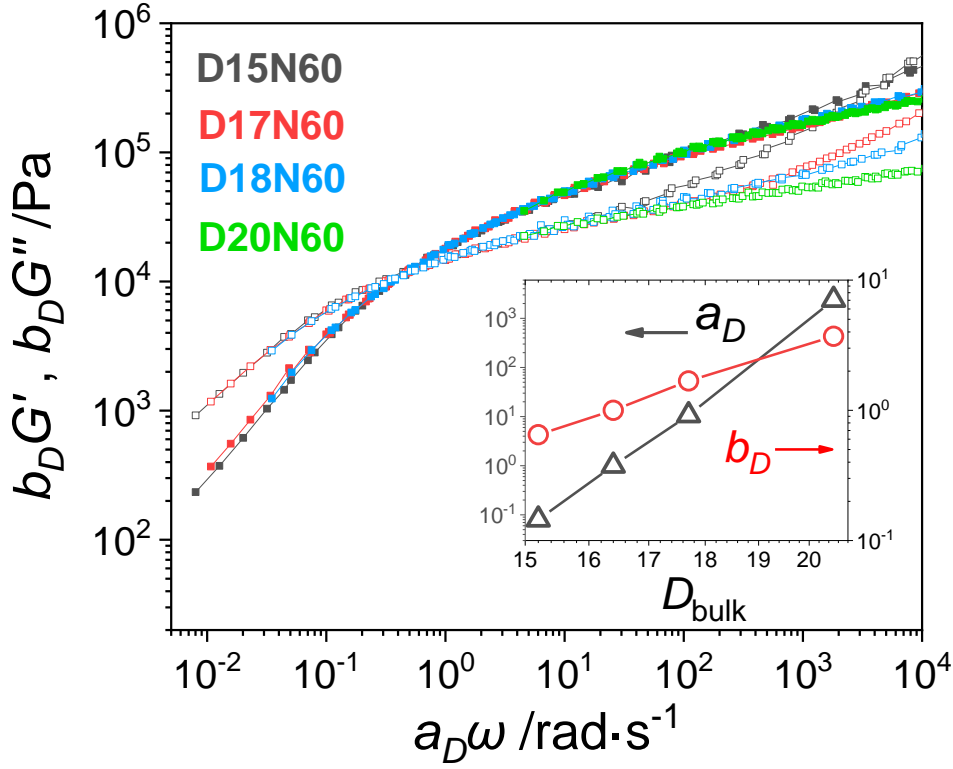


Figure S8. The master curves are based on a superposition of the low-frequency crossover point of the moduli. The inset plot is the corresponding shift factor.

(1) As mentioned above, a D_{bulk} -dependence could be seen according to b_D . The vertical shift factor b_D is the inverse reduced modulus.

$$b_D \sim \frac{1}{G_{\text{co,LF}}} \sim D_{\text{bulk}}^{5.9}$$

(2) Although D20N60 seems to be superposed and a corresponding a_D could be obtained, it doesn't mean D20N60 is relaxable at the corresponding time scale of a_D , because the validity of superposition is only assumed. Besides, the result of the creep test of D20N60 has confirmed there's no relaxation within 10000s at 200 °C.

(3) The spectra of SNPs with similar D_{bulk} and different N_c show poor self-similarity to achieve superposition.

6. Creep data and converting into dynamic moduli

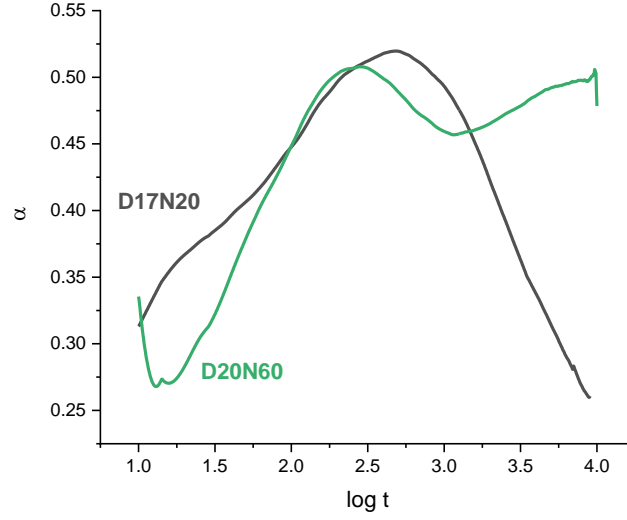


Figure S9. The slopes of creep compliance curves in log-log scale ($\frac{d \log J}{d \log t} - \log t$)

To converting the creep result into dynamic moduli, two numerical methods are commonly applied (a comprehensive introduction was presented in Cho's paper J. Rheol. – 60(2016), 1181):

(1) Mason's method (Rheol. Acta. – 39(2000), 371): An approximation based on the first-order Taylor expansion of the compliance $J(t)$ in log-log scale

$$\alpha(t) \equiv \frac{d \log J}{d \log t}$$

$$G'(\omega) + iG''(\omega) = \frac{1}{J(t)\Gamma[\alpha + 1]} \left(\cos \frac{\pi\alpha}{2} + i \sin \frac{\pi\alpha}{2} \right) \Big|_{t=\frac{1}{\omega}}$$

in which $\Gamma[x]$ is the Gamma function.

(2) Evan's method (also known as i-Rheo, Phys. Rev. E – 80(2009), 012501 & Phys. Chem. Chem. Phys. – 22(2020), 3839): for a data set of creep (t_k, J_k) and $k = 1, \dots, N$, over-sampled by interpolating with cubic spline in log-log scale,

$$\frac{i\omega}{G'(\omega) + iG''(\omega)} = i\omega J_0 + \sum_{k=1}^N \frac{J_k - J_{k-1}}{t_k - t_{k-1}} (e^{-i\omega t_{k-1}} - e^{-i\omega t_k}) + \frac{e^{-i\omega t_N}}{\eta}$$

in which $t_0 = 0$, J_0 is an extrapolating parameter at $t_0 = 0$, and η is another extrapolating parameter representing the steady-state viscosity. In this work, $J_0 = 0$, and $\eta = 1,000,000,000$.

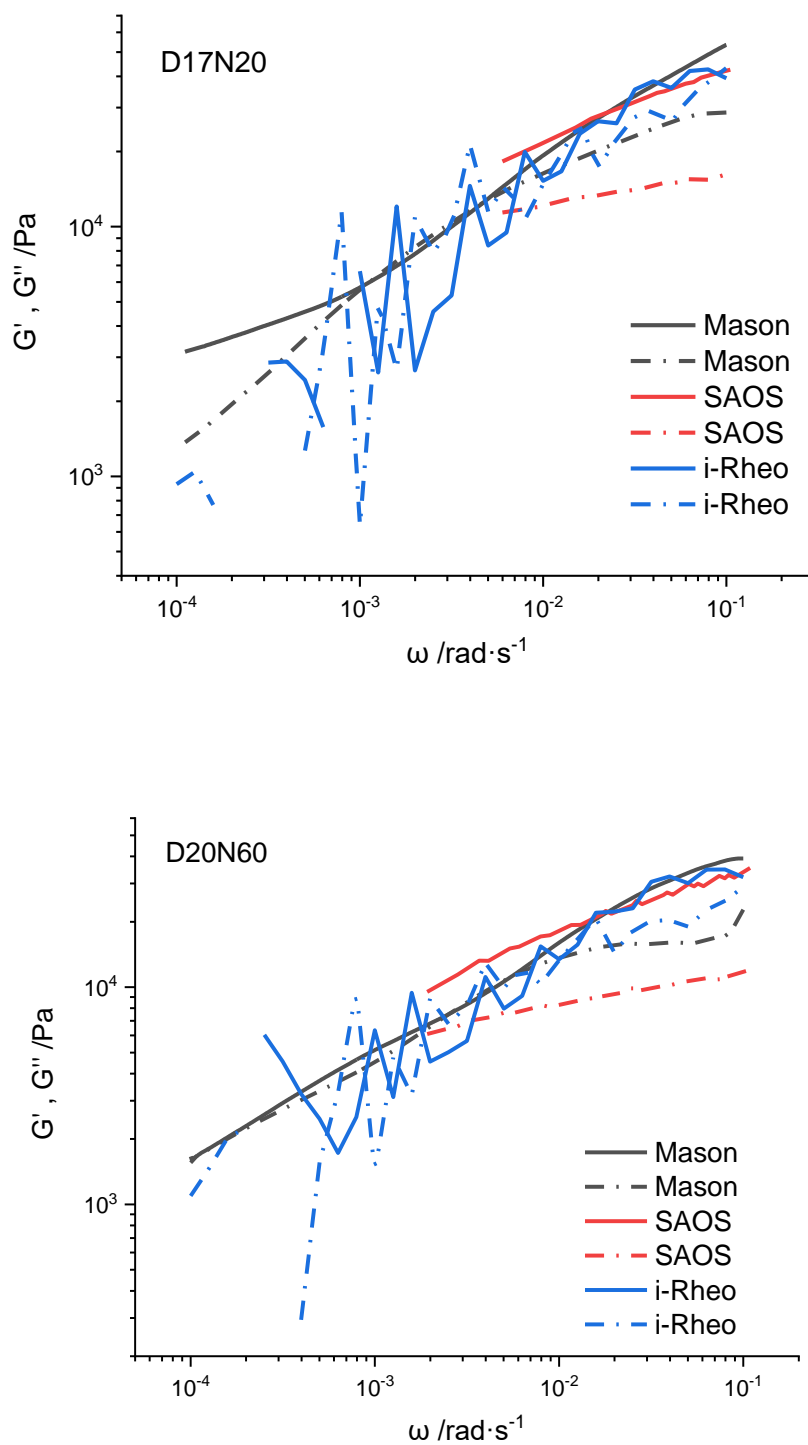


Figure S10. Moduli of D17N20 and D20N60 converted from creep compliance in Figure 4(d). Solid line: storage modulus; dashed line: loss modulus. Mason's method and Evan's method were applied respectively to get the black lines and blue lines (introduced above), comparing to the measured results of SAOS in red.

7. Degradation concerns

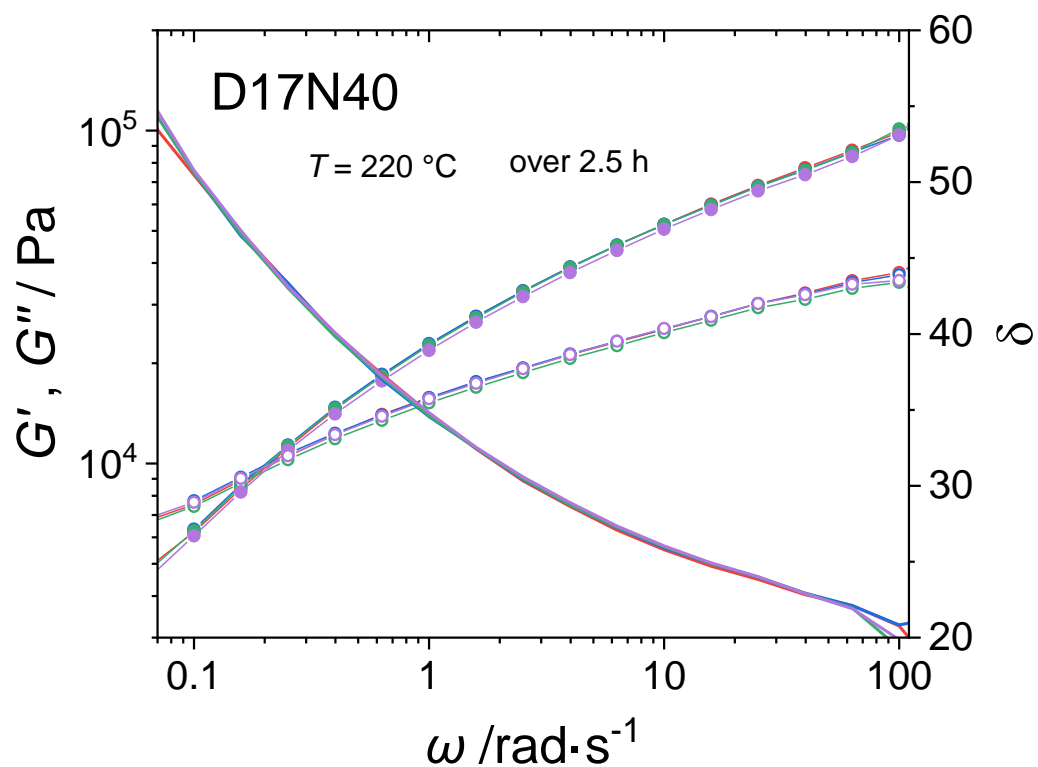


Figure S11. Comparison of the viscoelasticity of SNP (D17N40 as an example) during heating at 220 °C for more than 2 hours. There's no remarkable change of the spectrum, at least for the terminal relaxation.

Procedure

Test (~11min)–Wait (~37min) – Test(~11min) –Wait (~37min) – Test(~11min) – Wait (~37min) – Test (~11min)

8. Fitting of equation 12 in the lin-log scale of Figure 6

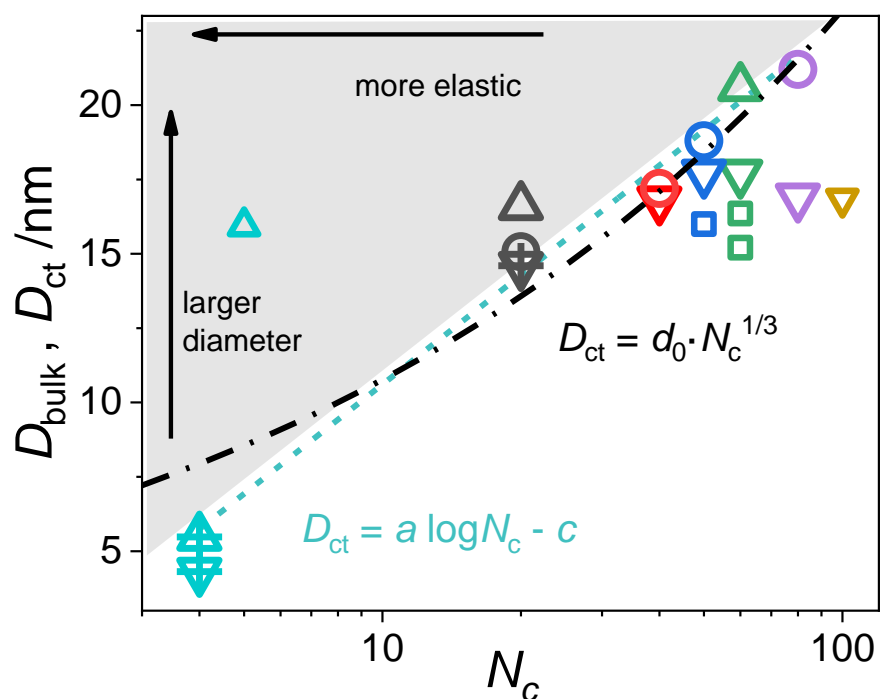


Figure S12. D_{ct} vs. N_c in lin-log scale. Circles are the fitting results of parameter D_{ct} by eq. (4). Triangles are measured data points. Upper triangles represent the upper limit of D_{ct} while lower triangles are the lower limit of D_{ct} . Symbols with a cross are literature data^{9, 14}. The cyan dashed line is fitted with six points (cyan upper triangle with a cross, green upper triangle, purple, blue, red, and gray circles) in the lin-log scale according to eq. (12).

9. Alternative fitting of Figure 5a against the effective volume and in log-lin scale

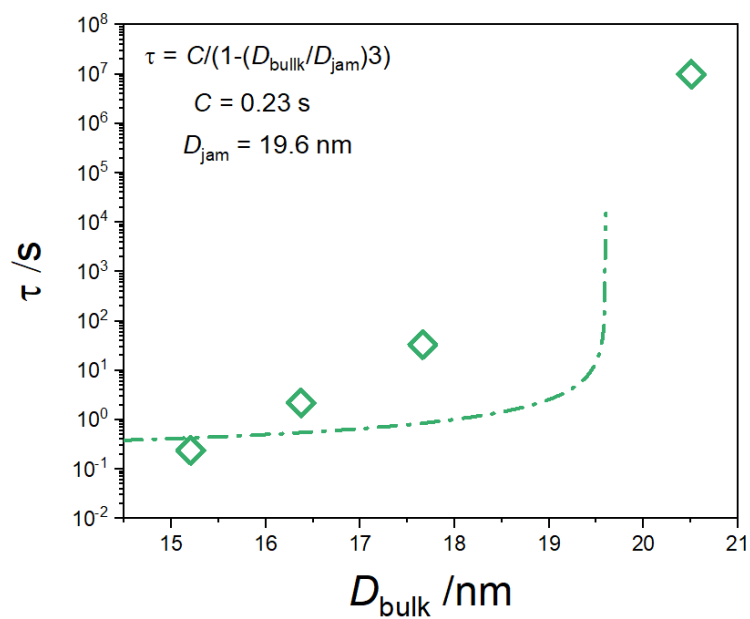


Figure S13. Four points with $N_c = 60$ cannot be simply fitted into the form of $\tau(D_{\text{bulk}}, D_{\text{ct}}) \propto 1/[1 - (D_{\text{bulk}}/D_{\text{ct}})^3]$. The τ of D20N60 is estimated by a lower limit.

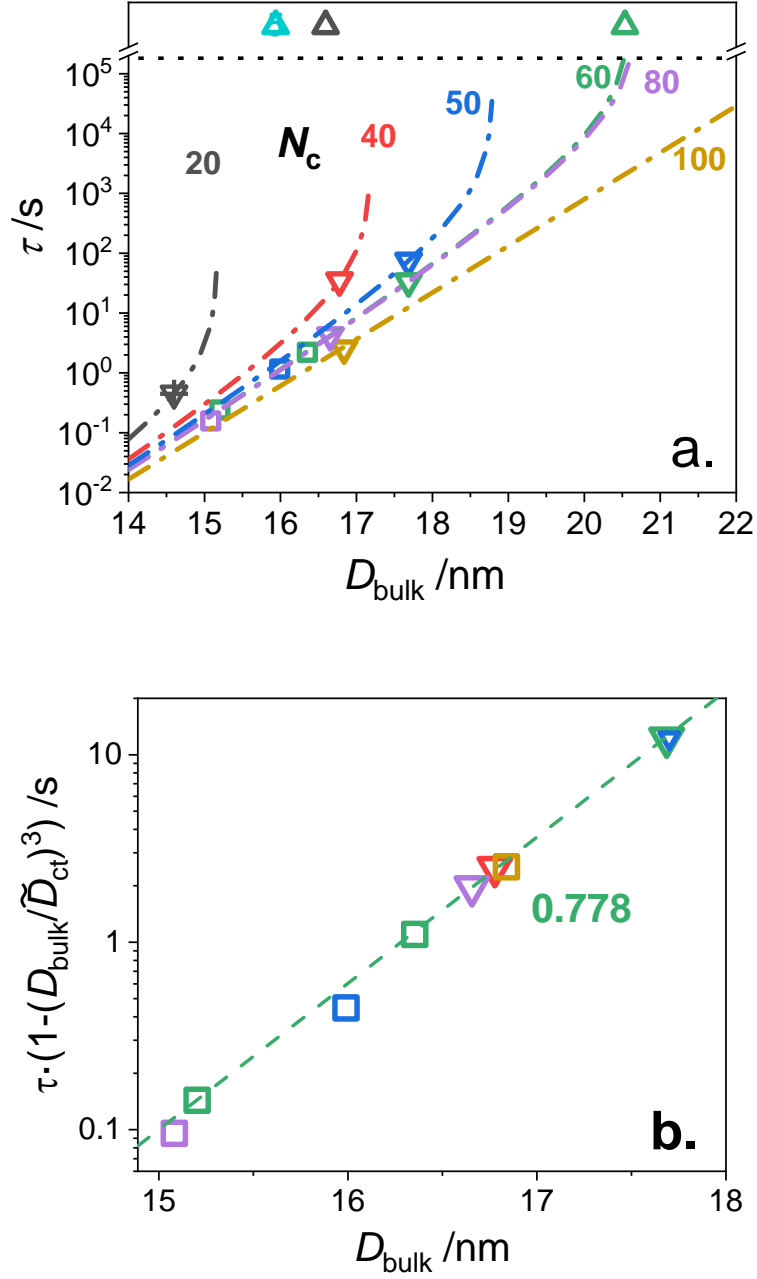


Figure S14. (a) Relaxation time v.s. D_{bulk} in log-lin scale. A fitting according to $\tau(D_{\text{bulk}}, N_c) = \tilde{A} \cdot 10^{\tilde{\alpha} D_{\text{bulk}}} \cdot h(D_{\text{bulk}}, N_c)$ has been performed, while $h(D_{\text{bulk}}, N_c)$ is also assumed as eq. (4). Following the same procedure of Figure 5a: (1) Assuming $\tilde{D}_{\text{ct}} = 20.6$ nm (D_{bulk} of D20N60) for the series $N_c = 60$ to get the universal parameters $\tilde{\alpha} = 0.778$ and $\tilde{A} = 10^{-12.7}$ by fitting series N_c 60; (2) to determine D_{ct} for each N_c by fitting each series with the same $\tilde{\alpha}$ and \tilde{A} . As a result, $\tilde{D}_{\text{ct}} = 15.2$, 17.2, 18.8, and 20.7 for N_c of 20, 40, 50, and 80 respectively. (b) Reduced relaxation time $\tau \cdot (1 - (D_{\text{bulk}}/\tilde{D}_{\text{ct}})^3)$ v.s. D_{bulk} to further confirm the fitting results.

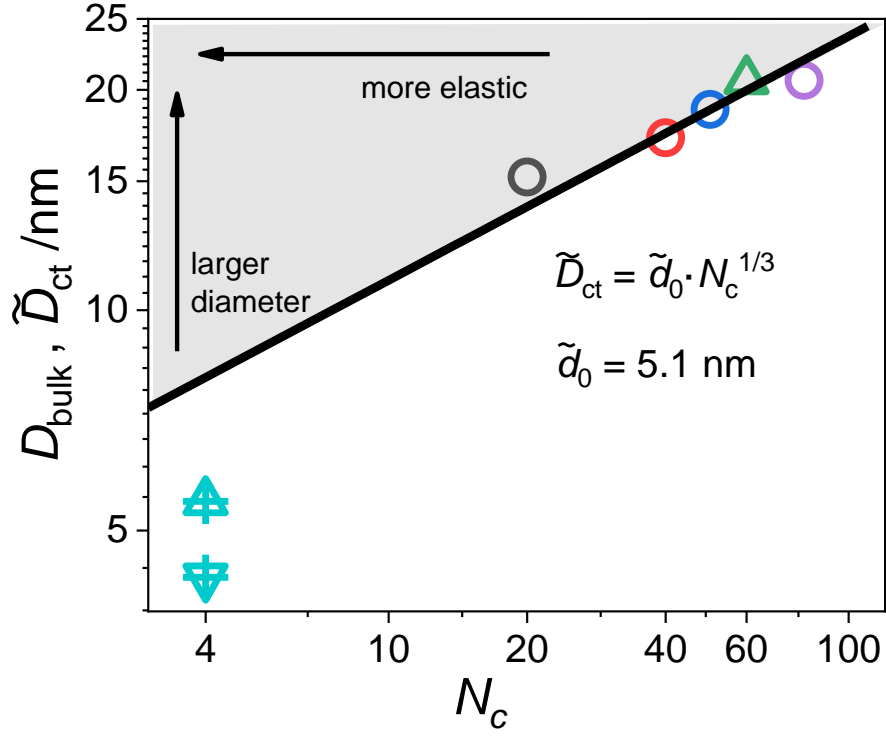


Figure S15. \tilde{D}_{ct} vs. N_c . in log-log scale. Four circles are the fitted \tilde{D}_{ct} from Figure S13. Symbols with a cross are literature data^{11, 16}. The black line is fitted to 5 points (green upper triangle, all four circles in purple, blue, red, and gray) in log-log scale to obtain $\tilde{d}_0 = 5.1$ nm according to eq. (9). It is shown that the evaluation of the critical diameter \tilde{D}_{ct} and \tilde{d}_0 is not sensitive to the details of the fitting approach.